

CHAPTER IV

RESULTS AND DISCUSSION

4.1 Adsorption Isotherm of CTAB on Aerosil[®]OX50

The CTAB adsorption isotherm on nonporous silica (Aerosil[®]OX50) shows three different regions (II, III, and IV) of the standard adsorption isotherm. The plateau region, representing the maximum adsorption of CTAB, is approximately 130 μmol of CTAB per gram of silica (see Figure 4.1) or 1.45 molecules/ nm^2 . The silica has a measured N_2 BET specific surface area of 53.8 m^2/g . If it is assumed that CTAB forms a perfect bilayer and completely covers the silica surface, the head of each CTAB molecule would cover 1.37 nm^2 on silica surface. However, the head group area of CTAB is 0.5 nm^2 (Thakulsukanant *et al.*, 1997). Therefore it is possible that there is electrostatic repulsion between adjacent CTAB head groups or CTAB does not completely cover the silica surface that is available to nitrogen.

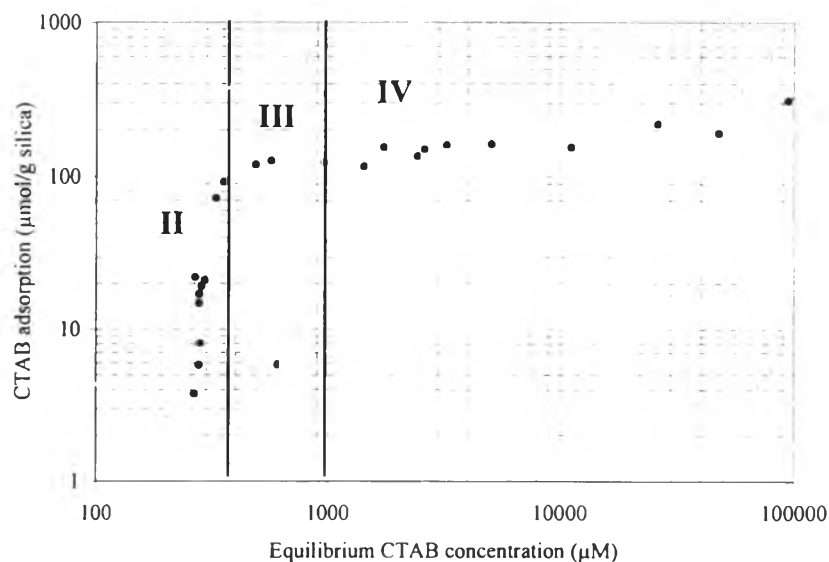


Figure 4.1 CTAB adsorption isotherm on Aerosil[®]OX50.

4.2 Styrene Adsolubilization

The adsolubilization of styrene into CTAB admicells on silica was investigated. The relationship between the amount of adsolubilized styrene and the equilibrium styrene concentration is shown in Figure 4.2 at two CTAB adsorption levels (20 and 100 $\mu\text{mol/g}$). As expected, when the equilibrium concentration of styrene increases, the amount of adsolubilized styrene increases. The amount of adsolubilized styrene at high surfactant adsorption was higher than low surfactant adsorption. The maximum measured styrene adsolubilization is ~ 190 $\mu\text{mol/g}$ of silica.

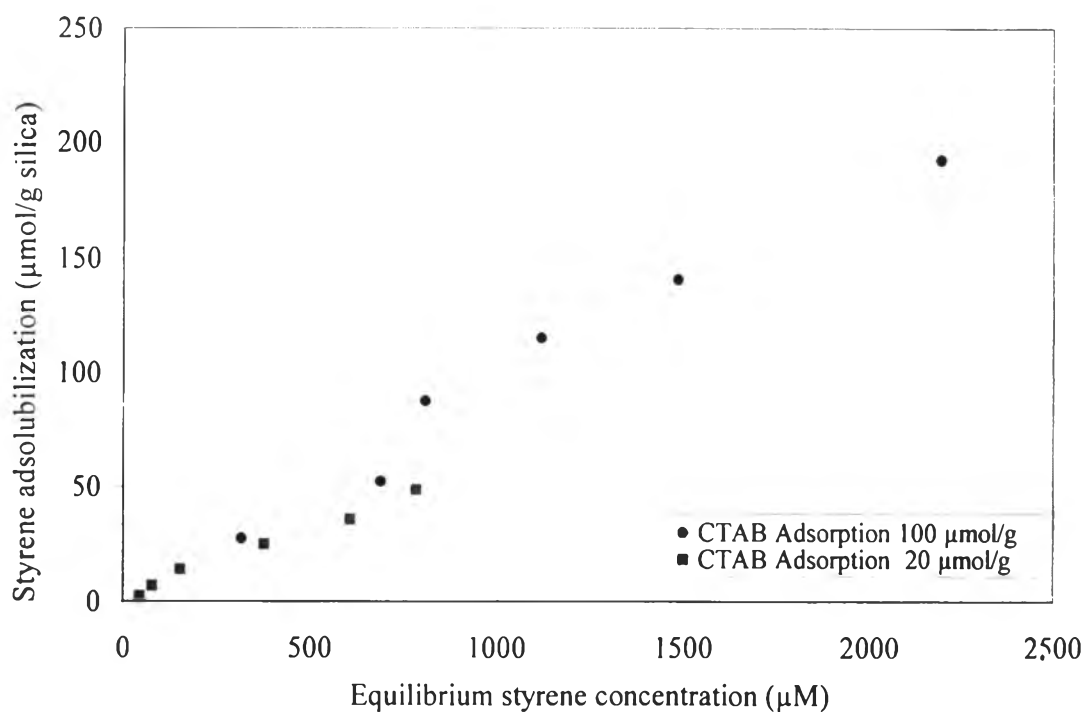


Figure 4.2 Adsolubilization isotherm of styrene at two CTAB adsorption (20 $\mu\text{mol/g}$ and 100 $\mu\text{mol/g}$).

4.3 Isoprene Adsolubilization

The adsolubilization of isoprene was determined and calculated from a mass balance method. The relationship between the amount of adsolubilized isoprene and the equilibrium isoprene concentration was shown in Figure 4.3. As expected, as the equilibrium concentration of isoprene increases the amount of adsolubilized isoprene increases. The maximum observed adsolubilization of isoprene is approximately 1200 $\mu\text{mol/g}$.

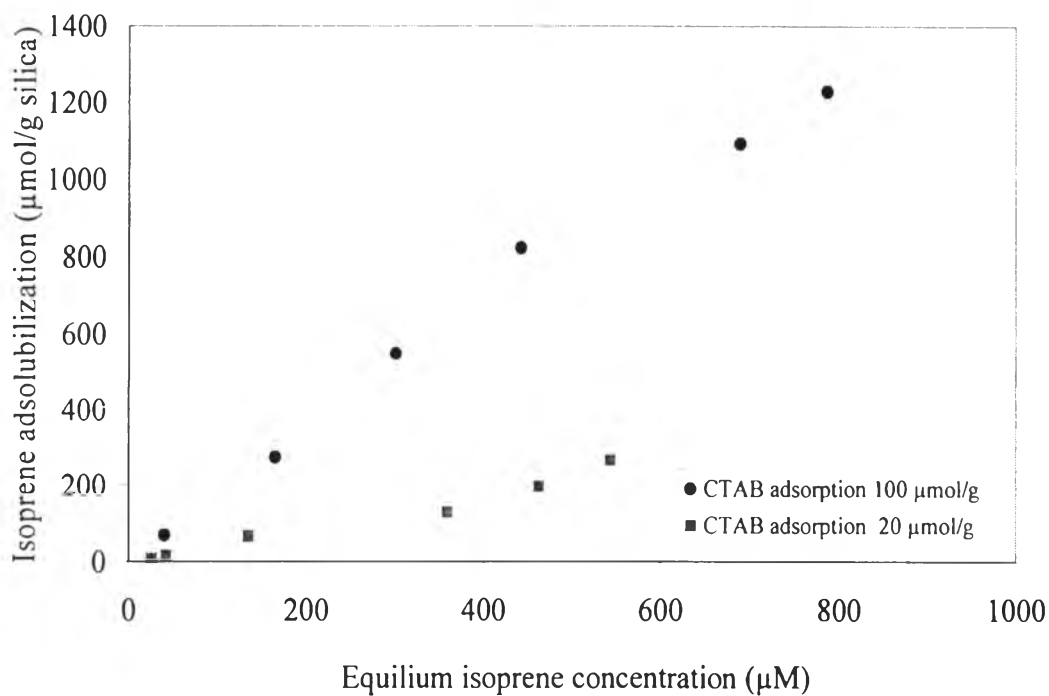


Figure 4.3 Adsolubilization isotherm of isoprene at two CTAB adsorption (20 $\mu\text{mol/g}$ and 100 $\mu\text{mol/g}$).

4.4 Admicellar Polymerization

The conditions of admicellar polymerization were set after the CTAB adsorption and monomer adsolubilization were investigated. The feed CTAB concentration was chosen such that the equilibrium concentration would be at approximately 80% of the CMC in order to avoid emulsion polymerization in the bulk. The experimental matrix for the preparation of ultra-thin polymer films is shown in Table 4.1.

Table 4.1 Admicellar polymerization condition

CTAB adsorption ($\mu\text{mol/g}$)	CTAB _{adsorp} : Comonomer _{adsol}		
	1 : 1	1 : 2	1 : 3
	CTAB _{adsorp} : Styrene _{adsol} : Isoprene _{adsol} ($\mu\text{mol/g}$) : ($\mu\text{mol/g}$) : ($\mu\text{mol/g}$)	CTAB _{adsorp} : Styrene _{adsol} : Isoprene _{adsol} ($\mu\text{mol/g}$) : ($\mu\text{mol/g}$) : ($\mu\text{mol/g}$)	CTAB _{adsorp} : Styrene _{adsol} : Isoprene _{adsol} ($\mu\text{mol/g}$) : ($\mu\text{mol/g}$) : ($\mu\text{mol/g}$)
20	20 : 5 : 15	20 : 10 : 30	20 : 15 : 45
	20 : 10 : 10	20 : 20 : 20	20 : 30 : 30
	20 : 15 : 5	20 : 30 : 10	20 : 45 : 15
100	100 : 25 : 75	100 : 50 : 150	100 : 75 : 225
	100 : 50 : 50	100 : 100 : 100	100 : 150 : 150
	100 : 75 : 25	100 : 150 : 50	100 : 225 : 75

4.5 Characterization of Modified silica, Extracted silica, and Extracted Copolymer

4.5.1 Fourier Transform Infrared Spectroscopy Results

In order to determine the presence of styrene-isoprene copolymer attached to the surface of the silica, the polymer formed on the modified silica sample was extracted by refluxing with tetrahydrofuran (THF). The presence of styrene-isoprene copolymer on silica particles was confirmed by FTIR after modification. Figure 4.4 shows the spectra of unmodified silica, modified silica, and extracted silica. Peaks of styrene-isoprene copolymer are not clearly represented in the spectrum of the modified silica. This is most likely due to the peaks of styrene-isoprene copolymer being interfered with the high intensity silica adsorption bands and the amount of copolymer coated on silica particles is very little when compared to the amount of silica. Therefore, after the modified silica was passed through the polymer extraction process, the extracted material was characterized by FTIR technique. The extracted material and the remaining silica after the extraction were analyzed by comparing the FTIR spectra obtained to the standard reference spectra of styrene-isoprene copolymer (Aldrich 18,292-3). The spectrum of extracted material for a ratio of styrene to isoprene 1:1 at CTAB adsorption 100 $\mu\text{mol/g}$ silica, is shown in Figure 4.5. The characteristic benzene ring functional group peak at 700 cm^{-1} proves the existence of styrene, and an aliphatic carbon double bond (C=C) peak at 1600 cm^{-1} confirm the presence of isoprene. An amino group peak (from CTAB) at 1500 cm^{-1} and silicon dioxide peak at 1100-1200 cm^{-1} are also found. The presences of these characteristic peaks suggest that styrene-isoprene copolymer was formed on the silica surface.

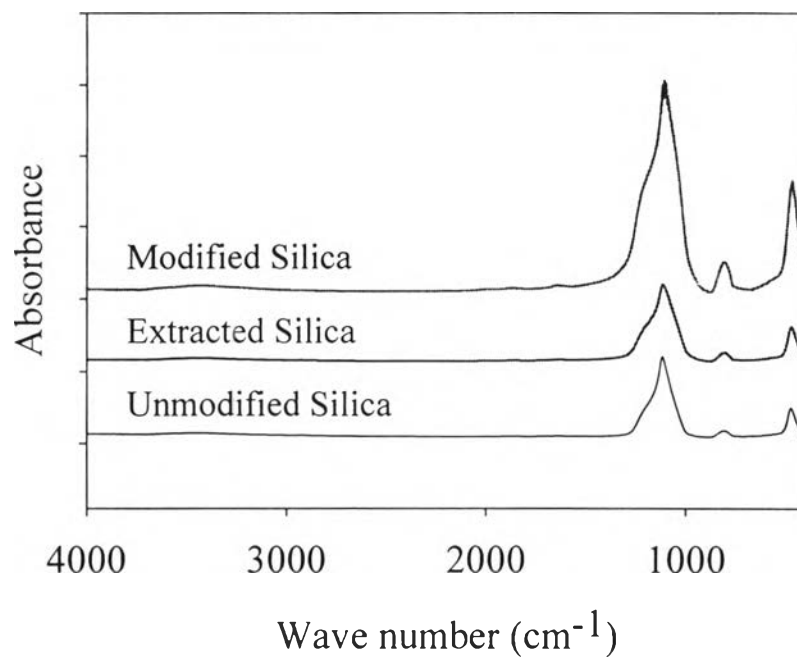


Figure 4.4 FTIR spectrum of unmodified silica, modified silica, and extracted silica.

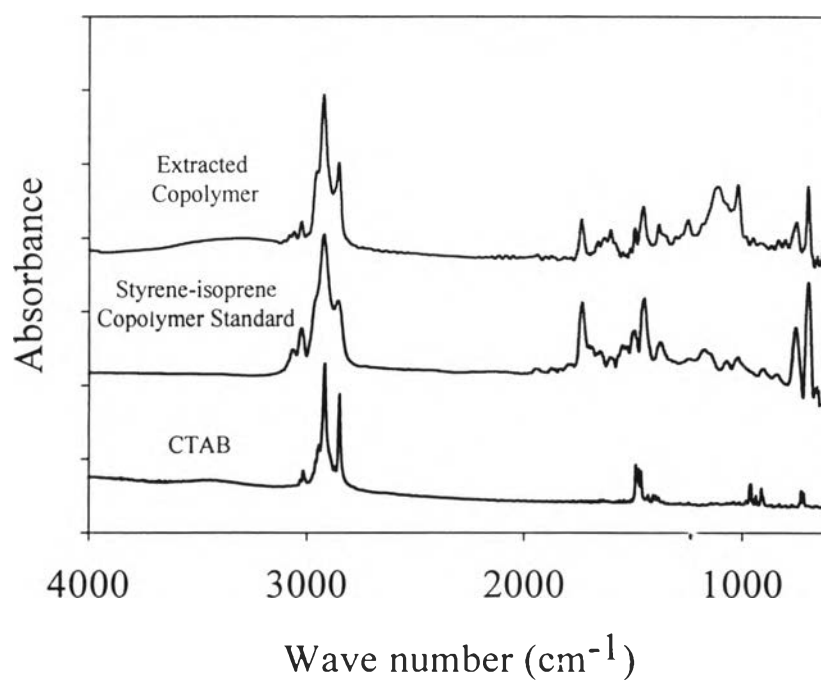


Figure 4.5 FTIR spectrum of CTAB, styrene-isoprene copolymer standard, and extracted copolymer.

4.5.2 Thermal Gravimetric Analysis Results

All samples were examined by thermogravimetric analysis in order to further verify the existence of styrene-isoprene copolymer formed on the silica surfaces. The TGA results of modified silicas before and after THF extraction show a two-step decomposition process (Figure 4.6). The first weight loss is the CTAB decomposition at 200-300°C (see Figure 4.7). The second weight loss is due to styrene-isoprene copolymer decomposition at 300 to 500°C. Figure 4.8 shows the decomposition of extracted styrene-isoprene copolymer at ~400°C. Silica does not show any weight loss in this temperature range (see Figure 4.9). The extracted silica shows less significant weight loss between 300 and 500°C compare to modified silica one, as we expected (Figure 4.6). These provide evidence that most of the styrene-isoprene copolymer is extracted from the modified silica.

The quantity of formed copolymer can be studied from the percent weight loss of TGA results. All the mass losses were evaluated on the second degradation step at temperatures >300°C. TGA analysis of the results for modified silica, extracted silica and extracted polystyrene confirm that styrene-isoprene copolymer is successfully formed on the silica surface together with CTAB surfactant.

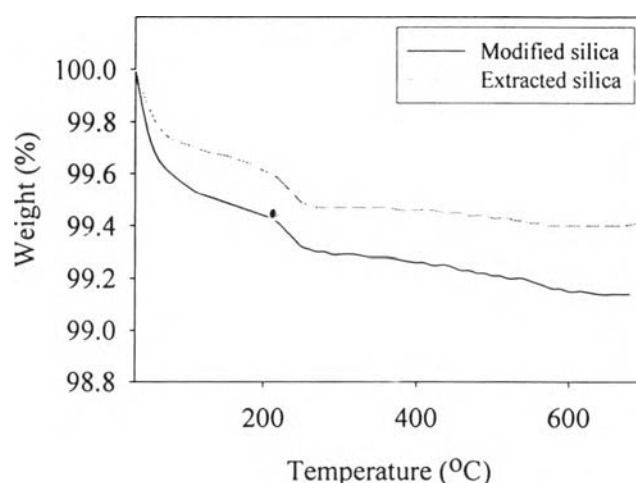


Figure 4.6 Thermal analysis of modified silica and extracted silica.

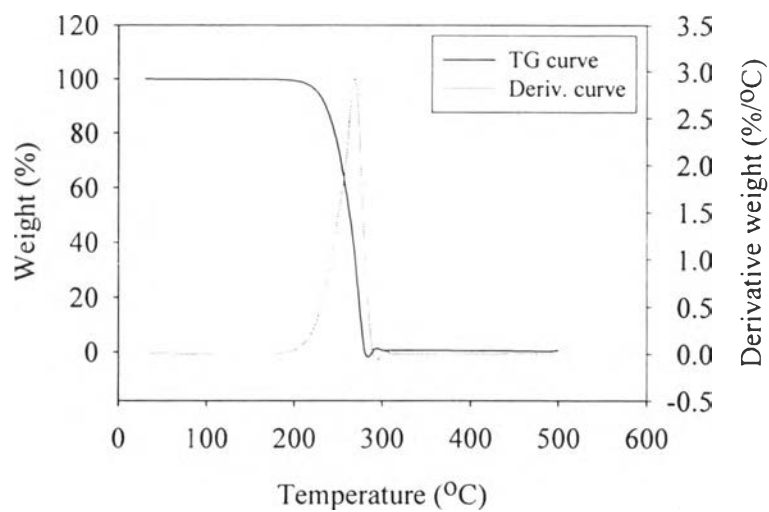


Figure 4.7 Thermal analysis of CTAB.

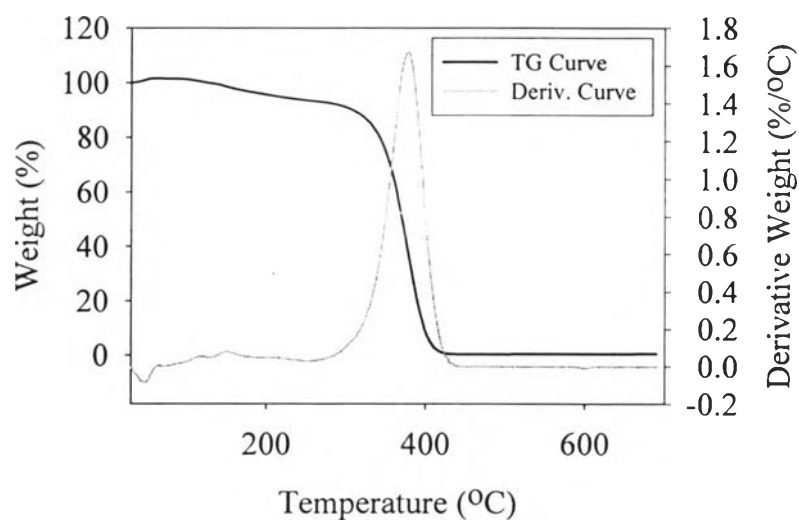


Figure 4.8 Thermal analysis of extracted styrene-isoprene copolymer.

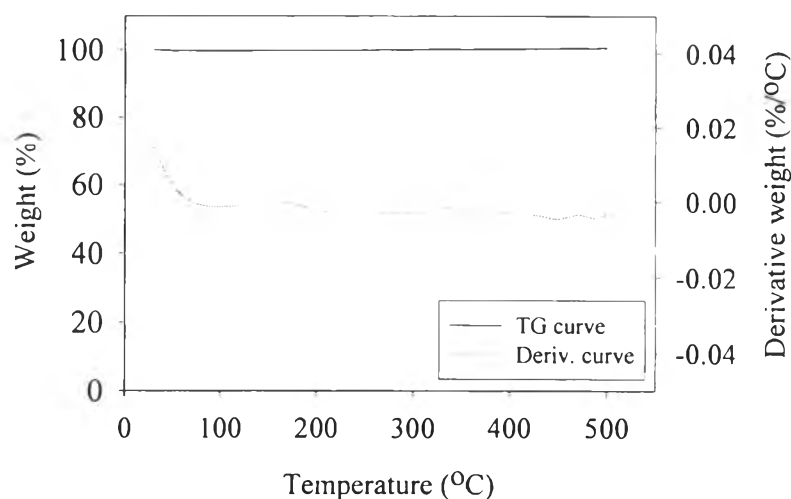


Figure 4.9 Thermal analysis of pure silica.

4.5.3. Gel Permeation Chromatography Results

The impact of comonomer loading and the comonomer ratio on the molecular weight of the formed film was determined by GPC using tetrahydrofuran as the solvent. Tables 4.2 and 4.3 show the number average molecular weight (\overline{M}_n), weight average molecular weight (\overline{M}_w), and molecular weight distribution (MWD) of the material extracted from modified silica. These modified silicas were produced from two different CTAB adsorptions (20 and 100 $\mu\text{mol/g}$) at different comonomer loadings and ratios of styrene to isoprene.

The GPC curves show two peaks, indicating two different ranges of molecular weight copolymer were obtained. The two peaks are in the ranges of weight average molecular weight (\overline{M}_w) between 1,300,000 to 47,000 gmol^{-1} , and 1200 to 900 gmol^{-1} . The first peak indicates high molecular weight styrene-isoprene copolymer while the second peak is probably due to lower molecular weight polymer and possibly some entrapped CTAB.

The copolymer in the higher MW range is probably due to polymerization within monomer-rich regions within the admicelle (See and O'Haver, 2004). Monomers in the swollen regions would have a high concentration and would not have to travel far to participate in the reaction. The copolymer in the lower M_w range is probably formed by the competition between the propagation and

termination steps versus diffusion within and into the admicelle. As a chain is initiated propagation commences. As monomer is consumed, monomer from surrounding areas or from the bulk will diffuse into the region. These results suggest that in many cases approximately 8 to 10 monomers take part in a chain before termination occurs.

When comparing the polymer at the two different levels of CTAB adsorption, the results show that at the high level of CTAB adsorption (100 $\mu\text{mol/g}$ silica) the molecular weight of the formed copolymer is higher than at the low level of CTAB adsorption (20 $\mu\text{mol/g}$ silica). It must be remembered that the admicelle is probably "patchy" on the surfaces at the lower coverage, and perhaps so at the high coverage (see in Figure 4.10). Therefore some polymerizations will occur in small aggregates that do not contain sufficient monomer to form high molecular weight polymer. The patchy admicelle will have more exposure to water surrounding it and this should increase the rate of termination. Thus, to obtain high molecular weight polymer, a high level of CTAB adsorption is preferable. In the same way, high levels of monomer loading cause the expected increase in molecular weight.

Overall, the GPC results indicate that increasing comonomer loading causes an increase in copolymer molecular weight. High comonomer loading levels cause the CTAB bilayer to swell and the density of comonomer per CTAB molecule increases. The comonomers have more mobility to react within the swollen bilayer as well as having a high concentration. Accordingly, in the competition between diffusion and termination, high molecular weight copolymer can form in most cases.

The effect of the ratios of styrene to isoprene was also studied. At CTAB adsorption of 20 $\mu\text{mol/g}$, the polymer weight average molecular weight (\overline{M}_w) ranged between 1160 to 920 gmol^{-1} at different ratios of styrene and isoprene. This could be due to the small amount of surfactant molecules adsorbed on silica surface and thus the amount of adsolubilized monomer in the admicelle is low (Figure 4.10). It suggests that perhaps the comonomers were spread out within the admicelle and the chances for two monomers to collide were reduced and the formation of higher molecular weight polymer unlikely. At 100 $\mu\text{mol/g}$ CTAB adsorption, the results show that at the high concentration of styrene

(styrene:isoprene = 3:1), the admicelle can no longer maintain its flattened bilayer structure but swells to surround the phase-separated regions of styrene within it (see Figure 4.11a). Once this occurs, the solute-solute interactions have begun to dominate over solute-surfactant tail interactions. Hence, these styrene droplets serve as reaction sites that form polymer aggregates during admicellar polymerization. Meanwhile, it is thought that the isoprene is spreading out in the admicelle and forms low molecular weight of polymer. Thus, the molecular weight copolymer at a styrene to isoprene ratio of 3:1 offered the higher molecular weight because of the higher amount of polystyrene. Whereas, the copolymer ratio of 1:3 has lower molecular weight than the ratio 1:1 and 3:1. Although isoprene has higher adsolubilization in the admicelle and reactivity than styrene, isoprene is likely to penetrate into palisade region (Kitiyanan *et al.*, 1996). This makes it difficult to react with other monomers (see Figure 4.11b and 4.11c). Consequently, at ratio 1:3, lower molecular weight copolymer was formed.

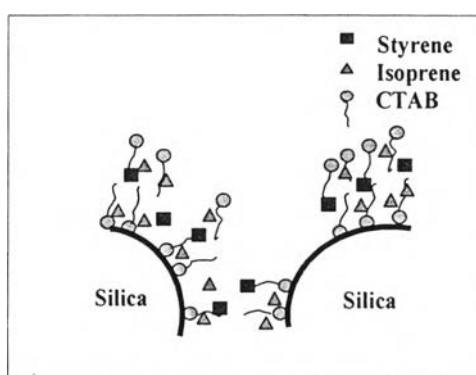
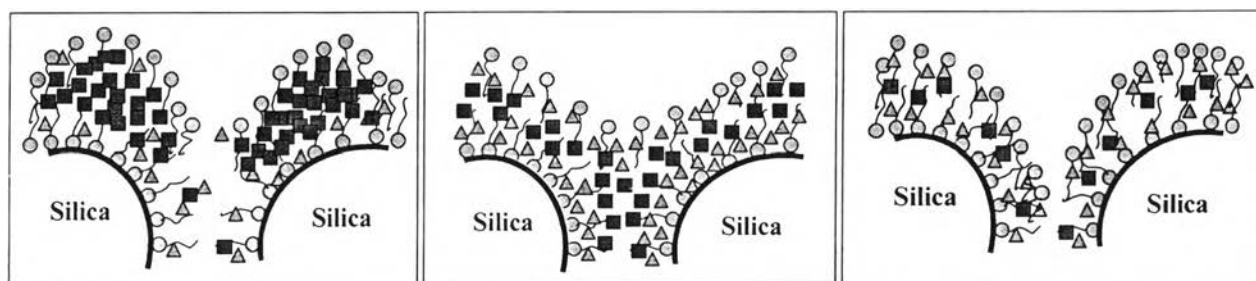


Figure 4.10 Structure model of adsolubilized styrene and isoprene monomers at CTAB adsorption 20 $\mu\text{mol/g}$.



where: \blacksquare Styrene, \triangle Isoprene, \odot CTAB

a) S : I = 3:1

b) S : I = 1:1

c) S : I = 1:3

Figure 4.11 Structure model of adsorbed styrene and isoprene monomers at CTAB adsorption $100 \mu\text{mol/g}$.

Table 4.2 \overline{M}_w , \overline{M}_n , and MWD of extracted materials produced in CTAB 20 $\mu\text{mol/g}$

CTAB _{adsorp} : Comonomer _{adsol} ($\mu\text{mol/g}$) : ($\mu\text{mol/g}$)	Ratio of styrene:isoprene	First peak			Second peak		
		\overline{M}_n	\overline{M}_w	MWD	\overline{M}_n	\overline{M}_w	MWD
1 : 1	1 : 3	-	-	-	675	930	1.38
1 : 2	1 : 3	-	-	-	738	1030	1.39
1 : 3	1 : 3	-	-	-	761	1090	1.43
1 : 1	1 : 1	-	-	-	669	923	1.38
1 : 2	1 : 1	-	-	-	792	1146	1.45
1 : 3	1 : 1	-	-	-	817	1156	1.41
1 : 1	3 : 1	-	-	-	707	972	1.37
1 : 2	3 : 1	-	-	-	733	995	1.36
1 : 3	3 : 1	-	-	-	708	1003	1.42

CTAB_{adsorp} = Adsorption of CTAB, ($\mu\text{mol/g}$), Comonomer_{adsol} = Adsolubilization of comonomer, ($\mu\text{mol/g}$)

Table 4.3 \overline{M}_w , \overline{M}_n , and MWD of extracted materials produced in CTAB 100 $\mu\text{mol/g}$

CTAB _{adsorp} : Comonomer _{adsol} ($\mu\text{mol/g}$) : ($\mu\text{mol/g}$)	Ratio of styrene:isoprene	First peak			Second peak		
		\overline{M}_n	\overline{M}_w	MWD	\overline{M}_n	\overline{M}_w	MWD
1 : 1	1 : 3	-	-	-	737	995	1.35
1 : 2	1 : 3	-	-	-	882	1,082	1.23
1 : 3	1 : 3	21,010	47,607	2.27	719	1,016	1.41
1 : 1	1 : 1	146,442	264,300	1.80	678	1,025	1.51
1 : 2	1 : 1	118,750	272,064	2.29	733	1,028	1.40
1 : 3	1 : 1	225,645	468,593	2.08	773	1,059	1.38
1 : 1	3 : 1	-	-	-	682	942	1.38
1 : 2	3 : 1	-	-	-	784	973	1.24
1 : 3	3 : 1	1,007,075	1,320,435	1.31	765	1,041	1.36

CTAB_{adsorp} = Adsorption of CTAB, ($\mu\text{mol/g}$), Comonomer_{adsol} = Adsolubilization of comonomer, ($\mu\text{mol/g}$)

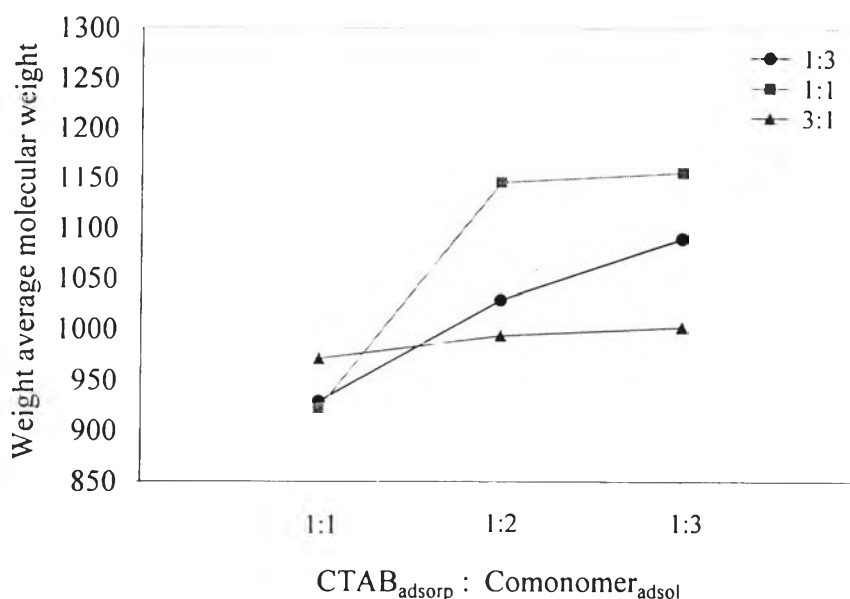


Figure 4.12 Effect of comonomer loading on weight average molecular weight on styrene-isoprene copolymer formed in CTAB adsorption 20 μ mol/g silica.

4.5.4. Atomic Force Micrograph of Modified Silica and Extracted Silica

All unmodified, modified and extracted silicas were studied by AFM in order to (1) determine the presence and characteristics of the formed copolymer thin film, and (2) determine the efficiency of the extraction process in removing the formed copolymer. Film thickness was measured using topographic images while confirmation of the presence of polymer can be obtained from comparing topographic and phase images. The effects of comonomer loading on the location and extent of the formed styrene-isoprene copolymer on the silica particles were also investigated using AFM.

In the same frame the result shows two types of image, topographic on the left and phase on the right. The topographic image of tapping mode image was interpreted by changing the oscillating amplitude of the tip during a tip tapped on the sample surface. The phase image can be used to interpret the hardness of sample surface. “Soft” samples will be seen as regions of darker contrast while hard areas will appear brighter in contrast. Thus, silica will appear light and polymer dark.

Figure 4.13 shows the atomic micrograph of unmodified silica. In phase mode, the valleys and edges of the primary particles appear darker, demonstrating that darker regions do not necessarily indicate softer regions on high surface area substrates. Thus, when darker areas were observed, imaging under different forces was used to determine if the region was polymer or not. As a result, the phase contrast in the valleys between the primary particles will appear to be darker, even without the presence of soft materials such as polymer films. It can be concluded that no polymer patches can be seen on the unmodified silica surface.

In Figure 4.14, a thin noncontinuous styrene-isoprene copolymer film is formed when the sample had 20 $\mu\text{mol/g}$ CTAB : 20 $\mu\text{mol/g}$ comonomer (1:3) at a styrene to isoprene ratio of 1:1. This film can be clearly distinguished as the darker areas in the phase image and the lighter regions in topographic image. These micrographs suggest that the CTAB bilayer (20 $\mu\text{mol/g}$) formed "islands-like" patches on the silica particles and that they were not entirely covering the surfaces of silica particles.

Figure 4.15 shows the atomic force micrograph of modified silica obtained in samples having 20 $\mu\text{mol/g}$ CTAB : 60 $\mu\text{mol/g}$ comonomer (1:3) at a styrene to isoprene ratio of 1:3. The micrograph results show pieces of smooth styrene-isoprene copolymer film coated on silica particles are clearly observed in the lighter regions of the topographic images. The styrene-isoprene copolymer films on the silica surface appeared as the dark regions in the phase image. These images show that copolymer thin films were formed in patches between silica particles.

Figure 4.16 shows the atomic force micrograph of modified silica obtained in systems containing 100 $\mu\text{mol/g}$ CTAB : 100 $\mu\text{mol/g}$ comonomer (1:1) at a styrene to isoprene ratio of 1:1. The micrograph shows that more copolymer can be seen (lighter regions) on the silica surface and between particles in the topographic image. From the phase image, styrene-isoprene copolymer, which corresponds to the darker regions, was formed around the edges of the silica particles.

Figure 4.17 shows the atomic force micrograph of modified silicas using a system of 100 $\mu\text{mol/g}$ CTAB : 200 $\mu\text{mol/g}$ comonomer (1:2) at a styrene to isoprene ratio of 1:1. The styrene-isoprene copolymer aggregates were scattered

around the coated silica surface as well as within the valleys between the primary silica particles.

Figure 4.18, 4.19, and 4.20 show the atomic force micrographs of modified silica obtained at 100 $\mu\text{mol/g}$ CTAB : 300 $\mu\text{mol/g}$ comonomer (1:3) and at styrene to isoprene ratios at 1:1, 1:3 and 3:1, respectively. Aggregates of styrene-isoprene copolymer on the silica surface were observed by topographic image. In the phase mode it is clear that the styrene-isoprene copolymer formed round droplets which sit on the silica and which nearly encapsulate the silica surface. These styrene-isoprene copolymer droplets confirm CTAB bilayer swelling at high levels of adsolubilized comonomer.

In addition the effects of comonomer loading on morphologies of styrene-isoprene copolymer formed on silica particles were investigated. At the low CTAB level (20 $\mu\text{mol/g}$), the morphology of styrene-isoprene copolymer formed on silica particles is compared in Figure 4.14 and 4.15. The results show that as the amount of copolymer increased, the styrene-isoprene copolymer thin film appears as the darker region in the phase image (Figures 4.14 and 4.15). A similar trend was observed when the morphologies of styrene-isoprene copolymer formed at high CTAB level (100 $\mu\text{mol/g}$) were compared (Figures 4.16, 4.17 and 4.18).

The effects of CTAB loading on the morphology of the styrene-isoprene copolymer formed on silica particles were also investigated. The morphologies of styrene-isoprene copolymer on silica particles in the same ratio of comonomer loading (1:3) but different CTAB levels were compared in Figures 4.15 (CTAB 20 $\mu\text{mol/g}$) and 4.18 (CTAB 100 $\mu\text{mol/g}$). When CTAB adsorption increased, the area covered by the styrene-isoprene copolymer films on the silica particles also increased. This is clearly seen when the phase images of silica modified at a comonomer loading ratio of 1:3 at different CTAB concentrations in compared in Figures 4.15 (CTAB 20 $\mu\text{mol/g}$) and 4.18 (CTAB 100 $\mu\text{mol/g}$).

The AFM was also used to confirm that the extraction process was efficient in removing essentially the entire polymer formed. Figure 4.21 shows atomic force micrographs of modified silica before and after extraction. The result shows that the large styrene-isoprene copolymer droplets/films which were visible on

the unextracted silica surfaces were missing on the silica surfaces after extraction. This suggests that the polymer analysis is representative of the polymer formed.

From the AFM cross-section analysis can use for studying the thickness of the deposited copolymer films. The results show that the film formed on silica surface was approximately 2-6 nm, as shown in Fig.4.22, 4.23, and 4.24.

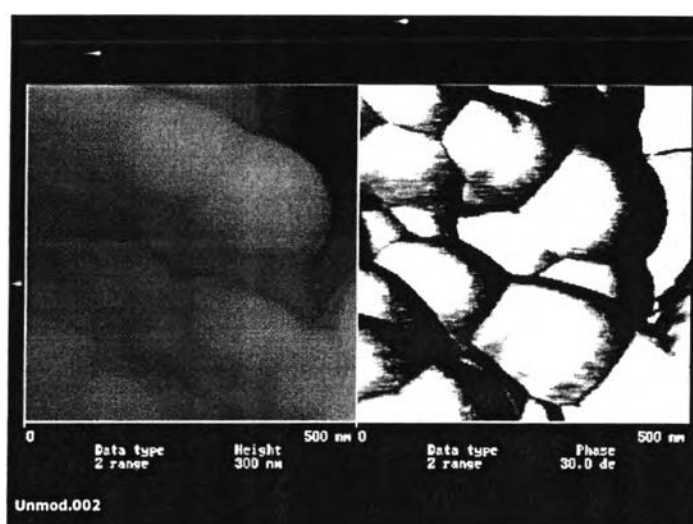


Figure 4.13 Atomic force micrograph of unmodified silica, Aerosil® OX50.

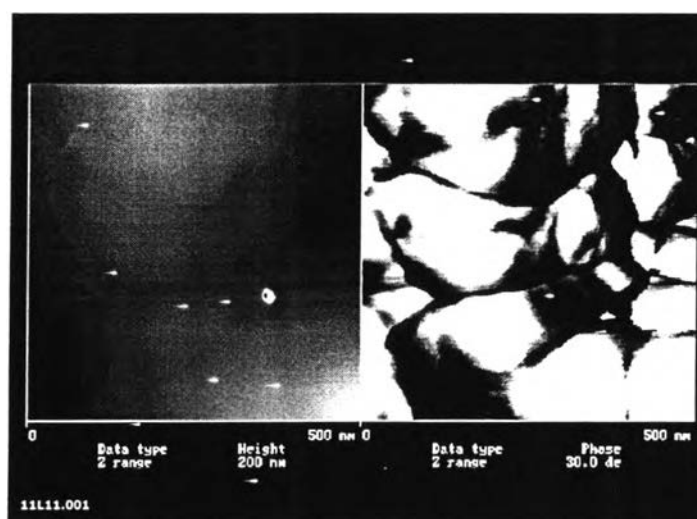


Figure 4.14 Atomic force micrograph of modified silica with adsorbed CTAB 20 μ mol/g : adsolubilized styrene 10 μ mol/g : adsolubilized isoprene 10 μ mol/g.

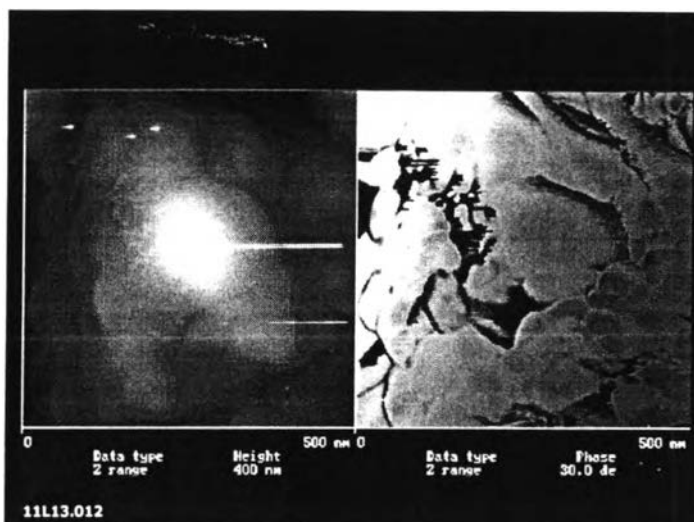


Figure 4.15 Atomic force micrograph of modified silica with adsorbed CTAB
 20 $\mu\text{mol/g}$: adsolubilized styrene 30 $\mu\text{mol/g}$: adsolubilized isoprene 30 $\mu\text{mol/g}$.

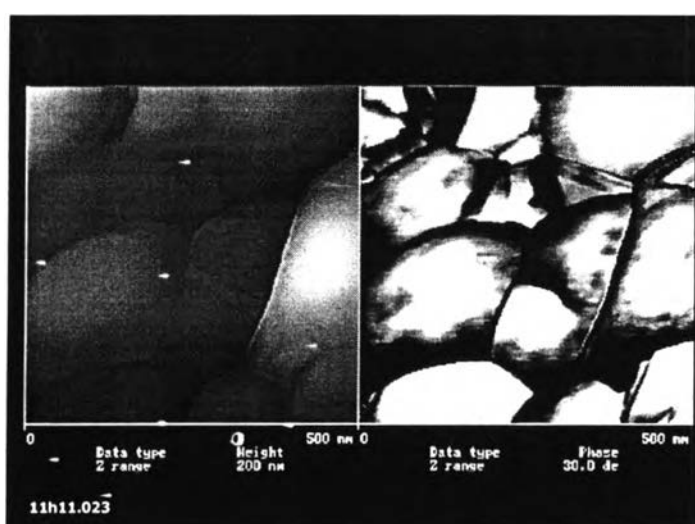


Figure 4.16 Atomic force micrograph of modified silica with adsorbed CTAB
 100 $\mu\text{mol/g}$: adsolubilized styrene 50 $\mu\text{mol/g}$: adsolubilized isoprene 50 $\mu\text{mol/g}$.

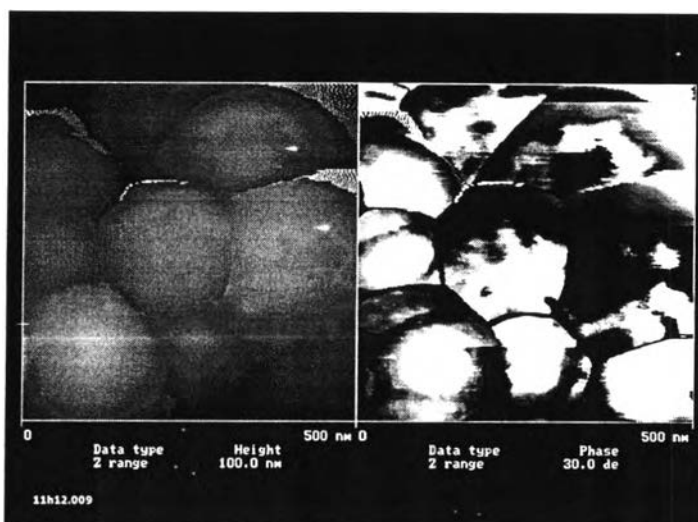


Figure 4.17 Atomic force micrograph of modified silica with adsorbed CTAB
 100 $\mu\text{mol/g}$: adsolubilized styrene 100 $\mu\text{mol/g}$: adsolubilized isoprene 100 $\mu\text{mol/g}$.

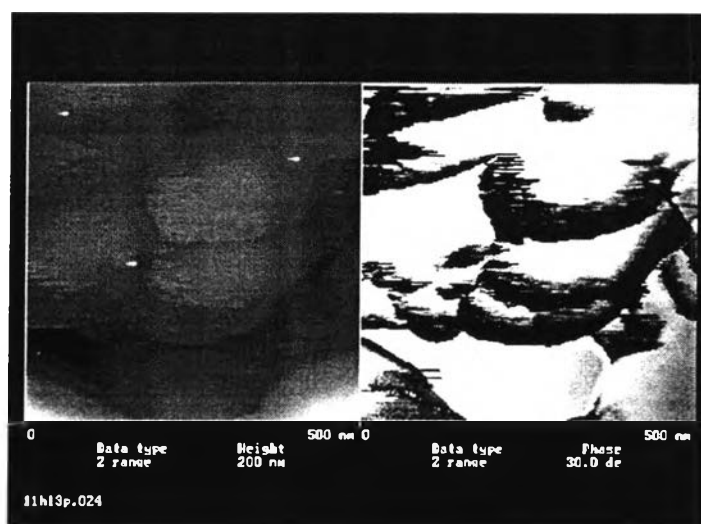


Figure 4.18 Atomic force micrograph of modified silica with adsorbed CTAB
 100 $\mu\text{mol/g}$: adsolubilized styrene 150 $\mu\text{mol/g}$: adsolubilized isoprene 150 $\mu\text{mol/g}$.

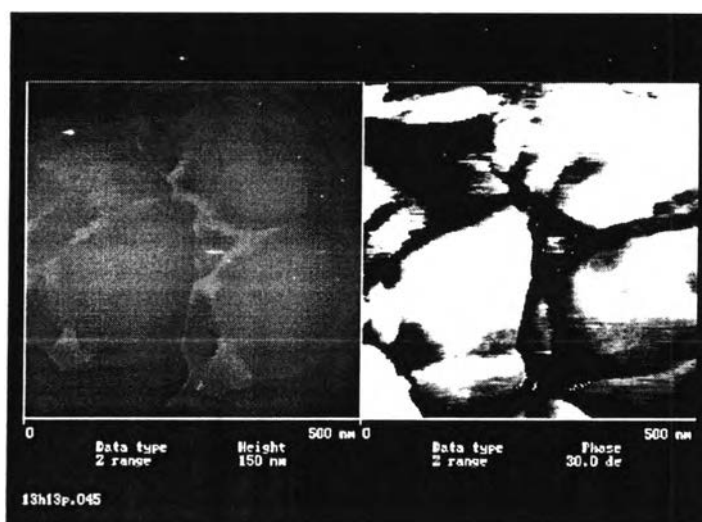


Figure 4.19 Atomic force micrograph of modified silica with adsorbed CTAB
 100 $\mu\text{mol/g}$: adsolubilized styrene 75 $\mu\text{mol/g}$: adsolubilized isoprene 225 $\mu\text{mol/g}$.

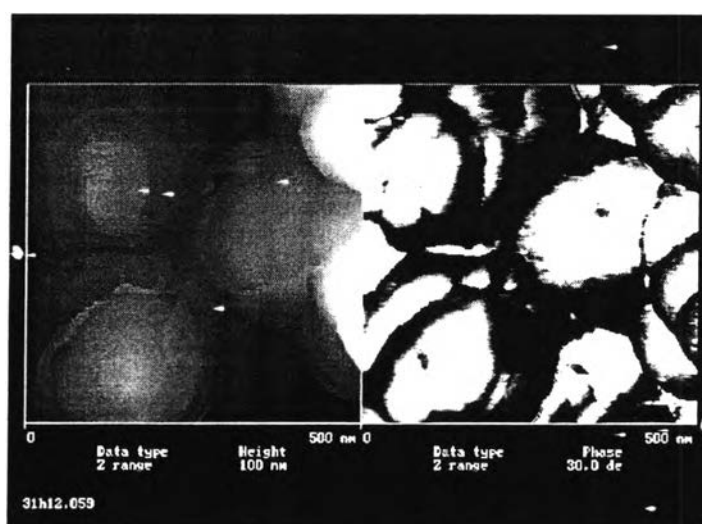
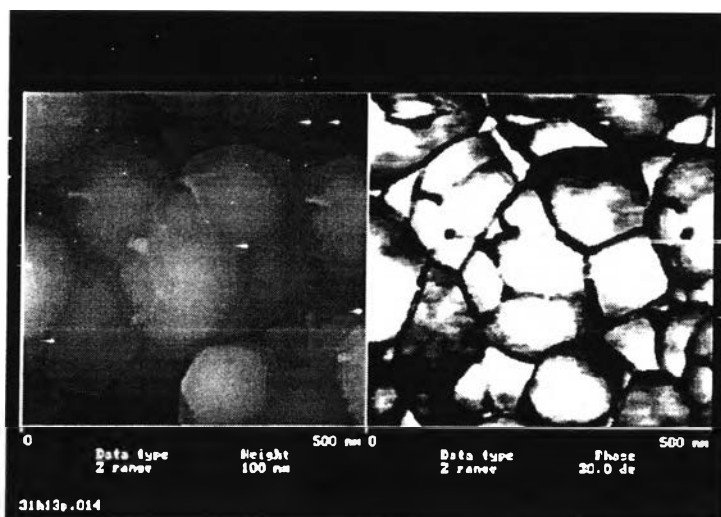
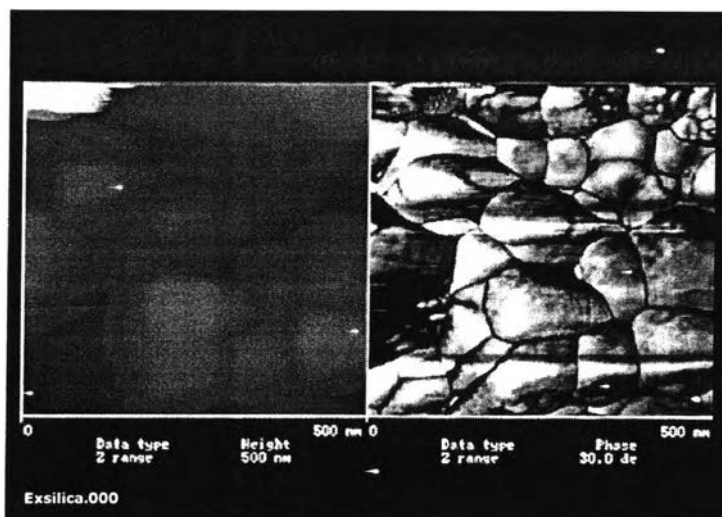


Figure 4.20 Atomic force micrograph of modified silica with adsorbed CTAB
 100 $\mu\text{mol/g}$: adsolubilized styrene 150 $\mu\text{mol/g}$: adsolubilized isoprene 50 $\mu\text{mol/g}$.



A. before extraction



B. after extraction

Figure 4.21 Comparison of atomic force micrograph of modified silica before and after extraction.

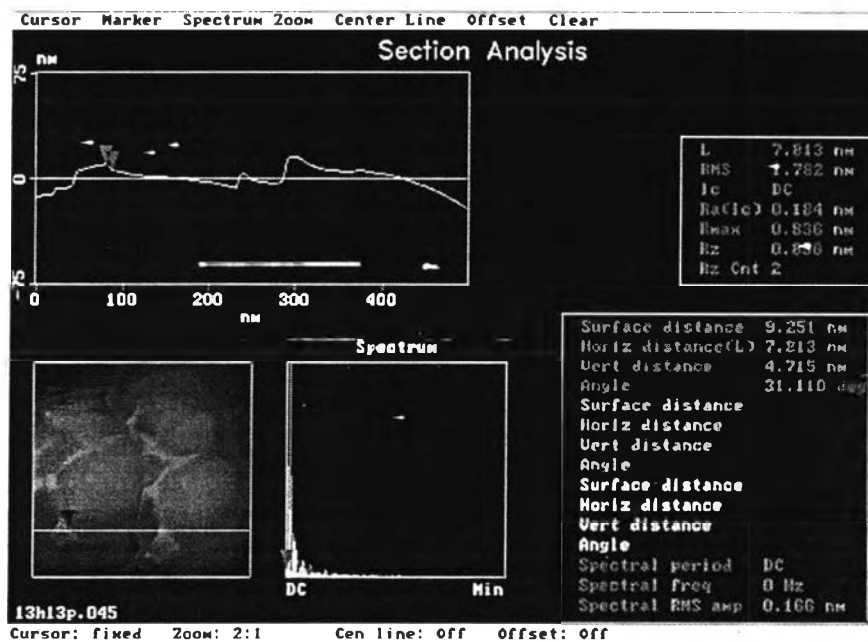


Figure 4.22 Thickness of styrene-isoprene film on modified silica with adsorbed CTAB 100 $\mu\text{mol/g}$: adsolubilized styrene 75 $\mu\text{mol/g}$: adsolubilized isoprene 225 $\mu\text{mol/g}$.

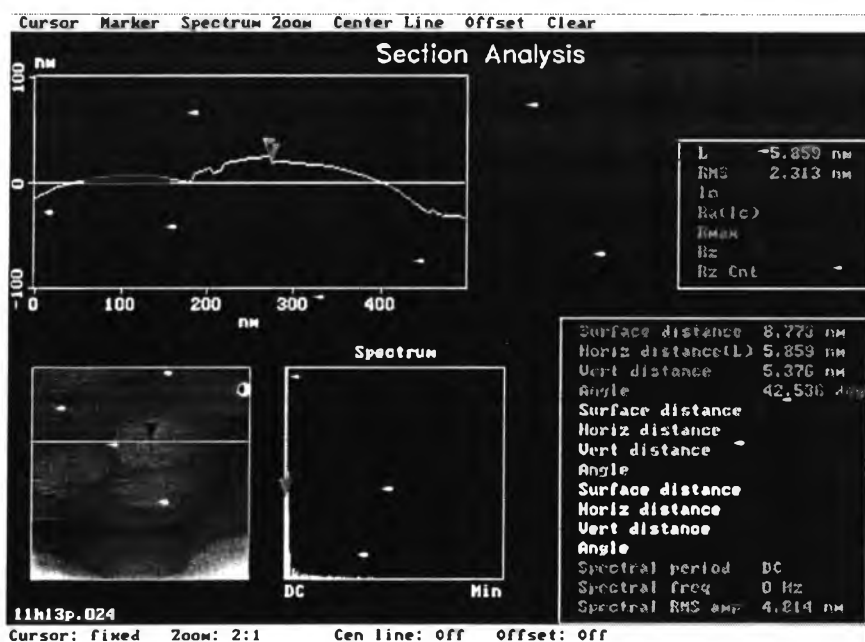


Figure 4.23 Thickness of styrene-isoprene film on modified silica with adsorbed CTAB 100 $\mu\text{mol/g}$: adsolubilized styrene 150 $\mu\text{mol/g}$: adsolubilized isoprene 150 $\mu\text{mol/g}$.

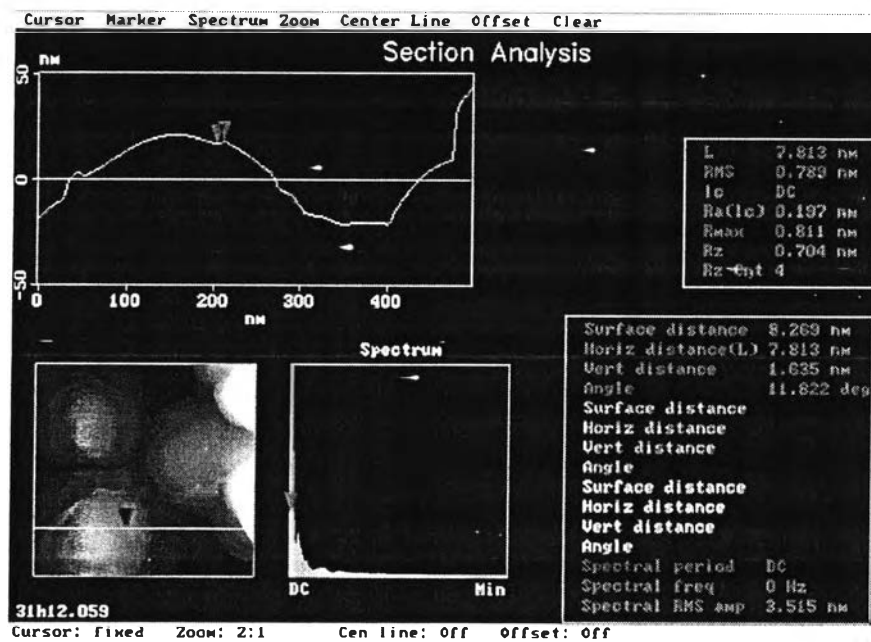


Figure 4.24 Thickness of styrene-isoprene film on modified silica with adsorbed CTAB 100 $\mu\text{mol/g}$: adsolubilized styrene 150 $\mu\text{mol/g}$: adsolubilized isoprene 50 $\mu\text{mol/g}$.